games

MDPI

Article

The Influence of Mobility Rate on Spiral Waves in Spatial Rock-Paper-Scissors Games

Mauro Mobilia *, Alastair M. Rucklidge and Bartosz Szczesny

Department of Applied Mathematics, School of Mathematics, University of Leeds, Leeds LS2 9JT, UK; A.M.Rucklidge@leeds.ac.uk (A.M.R.); bszcz@bszcz.org (B.S.)

* Correspondence: M.Mobilia@leeds.ac.uk; Tel.: +44-113-343-1591; Fax: +44-113-343-5090

Academic Editor: Attila Szolnoki

Received: 5 August 2016; Accepted: 31 August 2016; Published: 9 September 2016

Abstract: We consider a two-dimensional model of three species in rock-paper-scissors competition and study the self-organisation of the population into fascinating spiraling patterns. Within our individual-based metapopulation formulation, the population composition changes due to cyclic dominance (dominance-removal and dominance-replacement), mutations, and pair-exchange of neighboring individuals. Here, we study the influence of mobility on the emerging patterns and investigate when the pair-exchange rate is responsible for spiral waves to become elusive in stochastic lattice simulations. In particular, we show that the spiral waves predicted by the system's deterministic partial equations are found in lattice simulations only within a finite range of the mobility rate. We also report that in the absence of mutations and dominance-replacement, the resulting spiraling patterns are subject to convective instability and far-field breakup at low mobility rate. Possible applications of these resolution and far-field breakup phenomena are discussed.

Keywords: Rock-Paper-Scissors; cyclic dominance; pattern formation; spiral waves; diffusion; phase diagram; individual-based modelling; stochastic lattice simulations; complex Ginzburg-Landau equation

PACS: 87.23.Cc, 05.45.-a, 02.50.Ey, 87.23.Kg

1. Introduction

Understanding the mechanism allowing the maintenance of species coexistence is an issue of paramount importance [1]. Evolutionary game theory [2–4], where the success of one species depends on what the others are doing, provides a fruitful framework to investigate this question by means of paradigmatic schematic models. In this context, cyclic dominance is considered as a possible motif enhancing the maintenance of biodiversity, and models of populations in cyclic competition have recently received significant attention.

The rock-paper-scissors (RPS) game—in which rock crushes scissors, scissors cut paper, and paper wraps rock—and its variants are paradigmatic models for the cyclic competition between three species. Examples of RPS-like dynamical systems can be *Uta stansburiana* lizards, and communities of *E. coli* [5–9], as well as coral reef invertebrates [10]. In the absence of spatial degrees of freedom and mutations, the presence of demographic fluctuations in finite populations leads to the loss of biodiversity with the extinction of two species in a finite time, see, e.g., [11–16]. However, in nature, organisms typically interact with a finite number of individuals in their neighborhood and are able to migrate. It is by now well established both theoretically and experimentally that space and mobility greatly influence how species evolve and how ecosystems self-organize, see, e.g., [17–22]. Of particular relevance is the in vitro experiments with *Escherichia coli* of [5–8] showing that, when arranged on a Petri dish, three strains of bacteria in cyclic competition coexist for a long time while two of the species go

extinct when the interactions take place in well-shaken flasks. On the other hand, in vivo experiments of Ref. [23] with bacterial colonies in the intestines of co-caged mice have shown that mobility allows the bacteria to migrate between mice and to maintain their coexistence. These observations illustrate that *mobility can both promote and jeopardize biodiversity in RPS games*, as argued in Refs. [24–26]: In the experiments of Ref. [23], biodiversity is maintained only when there is migration, whereas in Ref. [6] species coexistence is lost in well-shaken flasks corresponding to a setting with a high mobility rate.

These considerations have motivated a series of studies aiming at investigating the relevance of spatial structure and individual's mobility on the properties of RPS-like systems. For instance, various two-dimensional versions of the model introduced by May and Leonard [27], characterized by cyclic "dominance removal" in which each species "removes" another in turn (see below), have received much attention [24–26,28–31]. It has been shown that species coexist for a long time in these models with pair-exchange among neighboring individuals: below a certain mobility threshold species coexist by forming intriguing spiraling patterns below a certain mobility threshold, whereas there is loss of biodiversity above that threshold [24–26]. Another popular class of RPS models are those characterized by a zero-sum cyclic interactions (via "dominance replacement") with a conservation law at mean-field level ("zero–sum" games) [32–40] and whose dynamics in two-dimensions also leads to a long–lasting coexistence of the species but not to the formation of spiraling patterns, see, e.g., [28,31,37]. Recent studies, see, e.g., [41–47], have investigated the dynamics of two-dimensional RPS models combining cyclic dominance removal and replacement, while various generalization to the case of more than three species have also been considered, see, e.g., [48–50]. In [43–47] we studied the spatio–temporal properties of a generic two–dimensional RPS-like model accounting for cyclic competition with dominance–removal and dominance–replacement, along with other evolutionary processes such as reproduction, mutation and mobility via hopping and pair–exchange between nearest neighbors. By adopting a metapopulation formulation and using a multiscale and size-expansion analysis, combined with numerical simulations, we analyzed the properties of the emerging spatio–temporaldynamics. In particular, we derived the system's phase diagram and characterized the spiraling patterns in each of the phases and showed how *non-linear mobility* can cause the far-field breakup of spiral waves. In spite of the predictions of the theoretical models, it is still unclear under which circumstances microbial communities in cyclic competition would self-arrange into spiraling patterns as those observed in other systems such as myxobacteria and slime molds [51,52].

Here, we continue our investigation of the generic two–dimensional RPS-like model of [43–45] by focusing on the influence of pair-exchange between nearest-neighbors, as simplest form of migration, on the formation of spiraling patterns in two-dimensional lattice simulations. In particular, we demonstrate a *resolution issue*: on a finite grid spiral waves can be observed only when the migration is within a certain range. We also show that in the absence of mutations and dominance-replacement, e.g., as in [24–26,41], the spiraling patterns emerging from the dynamics are subject to convective instability and far-field breakup at low mobility rate.

This paper is structured as follows: The generic metapopulation model [44,53] is introduced in Section 2 and, building on [43,45], the main features of its description at mean-field level and in terms of partial differential equations (PDEs) are outlined. Section 3 is dedicated to a summary of the characterization of the system's spiraling patterns in terms of the underlying complex Ginzburg-Landau equation (CGLE). Section 4 is dedicated to our novel results concerning the resolution issues in finite lattices and the far-field breakup and convective instability under low mobility. Finally, we conclude by summarizing and discussing our findings.

2. Model

As in [43,45], we consider the generic model of cyclic dominance between three competing species defined on an $L \times L$ periodic square lattice of patches, L being the linear size of the grid, where each node of the grid is labelled by a vector $\boldsymbol{\ell} = (\ell_1, \ell_2)$. As illustrated in Figure 1, each patch consists of

a well-mixed population of species S_1, S_2, S_3 and empty spaces $\emptyset$ and has a limited carrying capacity N: In each patch $\boldsymbol{\ell}$ there are therefore at most N individuals $N_i(\boldsymbol{\ell})$ of species S_i ($i = 1, 2, 3$), and there are also $N_\emptyset(\boldsymbol{\ell}) = N - N_{S_1}(\boldsymbol{\ell}) - N_{S_2}(\boldsymbol{\ell}) - N_{S_3}(\boldsymbol{\ell})$ empty spaces. Within each patch $\boldsymbol{\ell}$, the population composition evolves according to the most generic form of cyclic RPS according to the following schematic reactions:

$$S_i + S_{i+1} \xrightarrow{\sigma} S_i + \emptyset \qquad S_i + S_{i+1} \xrightarrow{\zeta} 2S_i \tag{1}$$

$$S_i + \emptyset \xrightarrow{\beta} 2S_i \qquad S_i \xrightarrow{\mu} S_{i\pm1}, \tag{2}$$

where the index $i \in \{1, 2, 3\}$ is ordered cyclically such that $S_{3+1} \equiv S_1$ and $S_{1-1} \equiv S_3$. The reactions (1) describe the generic form of cyclic competition, that comprises *dominance–removal* with rate σ and *dominance–replacement* with rate ζ [43,45,46]. The processes (2) allow for the reproduction of each species (with rate β) independently of the cyclic interaction provided that free space ($\emptyset$) is available within the patch. The biological interpretation of the mutations $S_i \to S_{i\pm1}$ (with rate μ) is, e.g., that they mimic the fact that side–blotched lizards *Uta stansburiana* undergo throat–color transformations [9], while from a mathematical perspective they yield a supercritical Hopf bifurcation at mean-field level, see [54,55], about which a multiscale expansion is feasible, see below and [43,45,46]. Since we are interested in analyzing the spatio–temporal arrangement of the populations, in addition to the intra–patch reactions (1)–(2), we also allow individuals to migrate between neighboring patches $\boldsymbol{\ell}$ and $\boldsymbol{\ell}'$ via pair exchange, according to

$$[X]_{\boldsymbol{\ell}}[Y]_{\boldsymbol{\ell}'} \quad \xrightarrow{\delta} \quad [Y]_{\boldsymbol{\ell}}[X]_{\boldsymbol{\ell}'}, \tag{3}$$

where $X \neq Y \in \{S_1, S_2, S_3, \emptyset\}$.

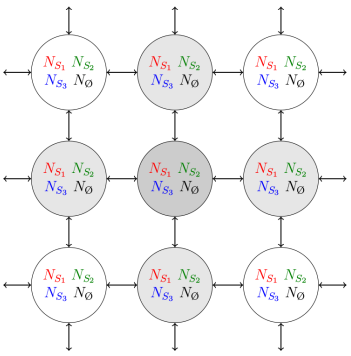

Figure 1. (Color online). Cartoon of the metapopulation model: $L \times L$ patches (or islands) are arranged on a periodic square lattice (of linear size L). Each patch $\boldsymbol{\ell} = (\ell_1, \ell_2)$ can accommodate at most N individuals of species S_1, S_2, S_3 and empty spaces denoted $\emptyset$. Each patch consists of a well–mixed population of N_{S_1} individuals of species S_1, N_{S_2} of type S_2, N_{S_3} of type S_3 and $N_\emptyset = N - N_{S_1} - N_{S_2} - N_{S_3}$ empty spaces. The composition of a patch evolves in time according to the processes (1) and (2). Furthermore, migration from the focal patch (dark gray) to its four nearest–neighbors (light gray) occurs according to the process (3), see text. Adapted from [45].

At an individual-based level, the model is defined by the Markov processes associated with the reactions (1)–(3). The model's dynamics is thus described by the underlying master equation, and the stochastic lattice simulations performed using the Gillespie algorithm [56], as explained in [43,45,47]. The metapopulation formulation of the model makes it well-suited for a size expansion of the master equation in $1/N$ [45,47,57–60]. Such an expansion in the inverse of the carrying capacity has been

detailed in Ref. [45] where we showed that to lowest order in the continuum limit ($L \gg 1$) on a square domain of size $\mathcal{S} \times \mathcal{S}$ the system evolves according to the partial differential equations

$$\partial_t s_i \;\; = \;\; D\Delta s_i + s_i[1-\rho-\sigma s_{i-1}] + \zeta s_i[s_{i+1}-s_{i-1}] + \mu\,[s_{i-1}+s_{i+1}-2s_i]\,, \tag{4}$$

with periodic boundary conditions, and where $s_i \equiv s_i(\boldsymbol{x},t)$, $\boldsymbol{x} = \mathcal{S}\ell/L$ is a continuous variable, and $\rho = s_1+s_2+s_3$. Here and henceforth, without loss of generality we have rescaled time by setting $\beta = 1$, and on average there are N microscopic interactions during a unit of time [45]. As usual, the diffusion coefficient D and the migration rate δ are simply related by $D = \delta(\mathcal{S}/L)^2$.

It is worth noting that contrary to the models of Refs. [43,45], here we do not consider non-linear diffusion: Movement in (4) appears only through the *linear diffusive terms* $D\Delta s_i$. Furthermore, while in Refs. [43,45] we focused on spatio-temporal patterns whose size exceeds that of the lattice unit spacing and we mostly considered domains of size $\mathcal{S} = L$ so that $D = \delta$, here we prefer to keep $\mathcal{S}$ and L separate, and therefore D and δ, distinct. Equation (4) are characterized by an interior fixed point $\boldsymbol{s}^* = (s_1^*, s_2^*, s_3^*)$ associated with the coexistence of the three species with the same density $s_i^* = s^* = 1/(3+\sigma)$. In the absence of space (i.e., upon setting $\Delta s_i = 0$ in (4)) and with no mutations ($\mu = 0$), $\boldsymbol{s}^*$ is never asymptotically stable and the mean field dynamics yields heteroclinic cycles (when $\mu = 0, \sigma > 0$ and $\zeta \geq 0$, with $\zeta = 0$ corresponding to the degenerate case) [27] or neutrally stable periodic orbits (when $\mu = \sigma = 0$ and $\zeta > 0$) [2–4] and finite-size fluctuations always lead to the quick extinction of two species [11–15]. However, quite interestingly when the mutation rate is non-zero, at mean-field level a supercritical Hopf bifurcation (HB) occurs at $\mu_H = \sigma/[6(3+\sigma)]$ and yields a stable limit cycle when $\mu < \mu_H$ [43] (see also [54,55]).

3. Spiraling Patterns and the Complex Ginzburg-Landau Equation

In [43,45] we showed that the dynamics in terms of the PDEs (4) yield spiraling patterns whose spatio-temporal properties can be analyzed in terms of the system underlying complex Ginzburg-Landau equation (CGLE) [62].

The latter is derived by introducing the "slow variables" $(\boldsymbol{X}, T) = (\epsilon\boldsymbol{x},\ \epsilon^2 t)$, where $\epsilon = \sqrt{3(\mu_H - \mu)}$ is the system's small parameter in terms of which a multiscale expansion is performed about the HB [61]. Details of the derivation can be found in Ref. [45] and brief accounts in [43,46]. Here we quote the system's CGLE for the complex modulated amplitude $\mathcal{A}(\boldsymbol{X}, T)$ which is a linear combination of the rescaled species densities [43,45,46]:

$$\partial_T \mathcal{A} = D\Delta_{\boldsymbol{X}}\mathcal{A} + \mathcal{A} - (1+ic)|\mathcal{A}|^2\mathcal{A}, \tag{5}$$

where $\Delta_{\boldsymbol{X}} = \partial^2_{X_1} + \partial^2_{X_2} = \epsilon^{-2}(\partial^2_{x_1} + \partial^2_{x_2})$ and $\partial_T = \epsilon^{-2}\partial_t$, and after having rescaled $\mathcal{A}$ by a constant, we find the parameter.

$$c = \frac{12\zeta(6-\sigma)(\sigma+\zeta) + \sigma^2(24-\sigma)}{3\sqrt{3}\sigma(6+\sigma)(\sigma+2\zeta)}. \tag{6}$$

As explained in [43,45], the CGLE (5) allows us to accurately characterize the spatio-temporal spiraling patterns in the vicinity of the HB (for $\epsilon \ll 1$ i.e., $\mu \lesssim \mu_H$) by using the well-known phase diagram of the two-dimensional CGLE, see, e.g., [62], and to gain significant insight into the system's spatio–temporal behavior away from the HB (we here restrict σ and ζ into [0,3]):

- For $\mu \lesssim \mu_H$ (close to the HB) [43]: There are four phases separated by the three critical values $(c_{\rm AI}, c_{\rm EI}, c_{\rm BS}) \approx (1.75, 1.25, 0.845)$, as shown in the phase diagram of Figure 2: No spiral waves can be sustained in the "absolute instability (AI) phase" ($c > c_{\rm AI} \approx 1.75$); spiral waves are convectively unstable in the Eckhaus instability (EI) phase with $c_{\rm EI} \approx 1.25 < c < c_{\rm AI}$; stable spiral waves are found in the bound state (BS) phase ($c_{\rm BS} \approx 0.845 < c < c_{\rm EI}$); while spiral waves annihilate when they collide in the spiral annihilation (SA) phase when $0 < c < c_{\rm BS}$.

- For $\mu \ll \mu_H$ (away from the HB) [45]: The AI, EI and BS phases are still present even away from the HB whose boundaries are essentially the same as in the vicinity of the HB, see Figure 3. At low mutation rate, there is no spiral annihilation and the SA phase is generally replaced by an extended BS phase (with far-field breakup of the spiral waves when $\sigma \gg \zeta$).

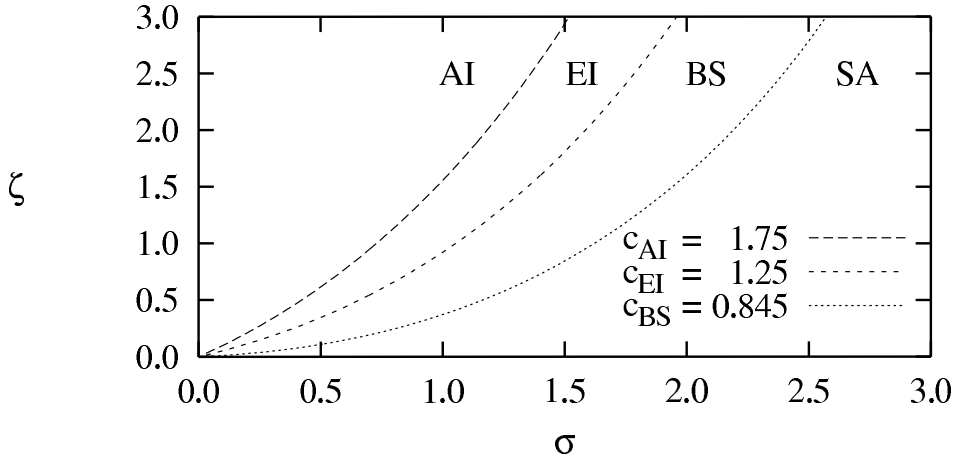

Figure 2. Phase diagram of the two–dimensional rock-paper-scissors (RPS) system around the Hopf bifurcation with contours of $c = (c_{\mathrm{AI}}, c_{\mathrm{EI}}, c_{\mathrm{BS}})$ in the $\sigma - \zeta$ plane, see text. We distinguish four phases: spiral waves are unstable in absolute instability (AI), Eckhaus instability (EI) and spiral annihilation (SA) phases, while they are stable in bound state (BS) phase. The boundaries between the phases have been obtained using the CGLE parameter (6). Adapted from [45].

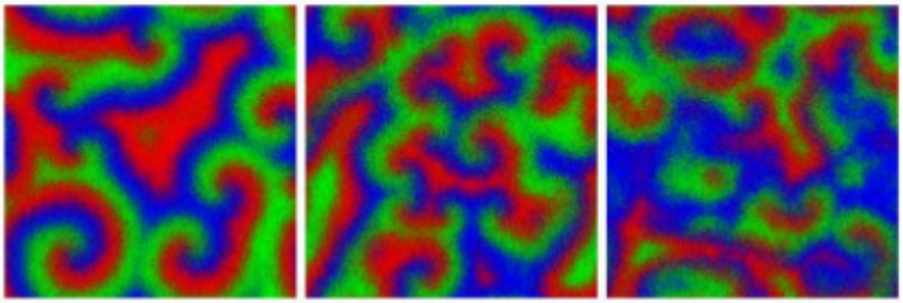

Figure 3. (Color online). Typical long-time snapshots in the BS (**left**), EI (**middle**) and AI (**right**) phases from stochastic simulations at low mutation rate. As in the next figures, each color represents one species (dark dots are regions of low density). The parameters are $L = 128$, $N = 64$, $(\beta, \sigma, \mu, \delta) = (1, 1, 0.001, 1)$, and $\zeta = 0.6$ (**left**), 1.2 (**middle**), and $\zeta = 1.8$ (**right**), see text. In all panels, the initial condition is a random perturbation of the homogeneous state $\boldsymbol{s}^*$, see text and [44]. Adapted from [47].

Away from the cores of the spiral waves, the solution to the CGLE (5) can be approximated by the travelling-wave ansatz $\mathcal{A}(\boldsymbol{X}, T) = Re^{i(\boldsymbol{k}\cdot\boldsymbol{X} - \omega T)}$ of amplitude $R(c)$, angular frequency ω and wave number $\boldsymbol{k}$ [45]. As detailed in Ref. [45], the wavelength $\lambda = 2\pi/(\epsilon k)$ of the spiraling patterns in the BS and EI phases near the HB in the physical space (in lattice units) can thus be estimated by $\lambda \approx \lambda_H$, where

$$\lambda_H = \frac{2\pi L}{\epsilon \mathcal{S}} \sqrt{\frac{D}{1 - R^2(c)}} = \frac{2\pi}{\epsilon} \sqrt{\frac{\delta}{1 - R^2(c)}}, \tag{7}$$

where the amplitude $R^2(c)$ is a decreasing function of c in the BS and EI phases (see Figure 6 in [45]) and has been found numerically to be in the range 0.84–0.95 in the BS phase [45].

In Ref. [45], we showed that the description in terms of the CGLE is not only valid and accurate near the HB ($\mu \lesssim \mu_H$), but it is also insightful in the limit $\mu \ll \mu_H$ of low mutation rate. In fact, we showed that lowering the mutation rate μ below μ_H results in three regimes: the AI, EI and BS phases, see Figure 3. We also found that reducing μ below μ_H results into shortening the wavelength λ of the spiraling patterns in the BS and EI phases: The wavelength at low mutation rate satisfies a linear relationship (see Figure 14 in Ref. [45]): $\lambda \approx \lambda_{\mu \ll \mu_H}$, where

$$\lambda_{\mu \ll \mu_H} = (\lambda_H - \lambda_0) \frac{\mu}{\mu_H} + \lambda_0, \tag{8}$$

where the wavelength λ_0 at $\mu = 0$ is inferred from the numerical solution of the PDEs (4) and is shorter than the wavelength λ_{μ_H} near μ_H; typically $\lambda_0 \in [0.3\lambda_{\mu_H}, 0.5\lambda_{\mu_H}]$ and it scales as $\lambda_0 \sim \sqrt{2\delta(3+\sigma)/\sigma}$ [63]. For instance, when $(\beta, \sigma, \zeta, \mu, \delta) = (1, 1, 0.6, 0.01, 0.64)$, we have $\epsilon \approx 0.308$, $R^2 \approx 0.9$ and (7) yields $\lambda_H \approx 52$ while we found $\lambda_0 \approx 26$ and therefore at $\mu = 0.01$, the wavelength is $\lambda_{\mu=0.01} \approx 32$ which is in good agreement with lattice simulations, see Figure 4 (bottom, left).

4. How Does Pair-Exchange Influence the Formation of Spiral Waves on a Grid?

We have seen that near the HB the RPS dynamics is generally well described in terms of the PDEs (4) and CGLE (5) when $N \gg 1$. Accordingly, the effect of space and individuals' mobility is accounted by linear diffusion. In this setting, rescaling the mobility rate $\delta \to \alpha\delta$ ($\alpha > 0$) boils down to rescale the diffusion coefficient and space according to $D \to \alpha D$ and $\boldsymbol{x} \to \boldsymbol{x}/\sqrt{\alpha}$. Hence, the size of the spatial patterns increases when the individuals' mobility is increased, and it decreases when the mobility is reduced [24–26,45]. Furthermore, according to the description in terms of the CGLE, the mobility rate and diffusion coefficient do not affect the stability of the spiraling patterns near the HB but only change their size. Below, we discuss the cases of very small or large mobility rate and show that this may result in spiral waves being elusive and/or unstable even in regimes where the PDEs (4) and CGLE (5) predict that they would exist and be stable.

4.1. Resolution Issues

In this section, we focus on resolution issues and show that while the description of the dynamics in terms of the PDEs (4) predict the formation of spiral waves these cannot be observed on finite lattice due to resolution issues. In other words, we report that, even when the PDEs (4) and CGLE (5) predict that the dynamics leads to stable spiraling patterns (BS phase), these may be elusive when the mobility rate is too low or too high as illustrated in Figure 4.

In order to determine the range of the mobility rate δ within which stable spiral waves can be observed on a two-dimensional grid, we distinguish three regimes, see Table 1: (i) $\lambda \sim o(1)$; (ii) $1 \ll \lambda \ll L$; (iii) $\lambda \gtrsim \mathcal{O}(L)$. In regime (i), the PDEs (4) predict a myriad of tiny spirals of wavelength of the order of one unit lattice space. Clearly, the resolution of any finite lattice is insufficient to allow to observe spiraling patterns of such a tiny size (of order of one pixel) on the grid, see Figure 4 (top). In this situation, instead of spiral waves lattice simulations lead to apparently clumps of activity. As shown in Figure 4, this phenomenon does not stem from demographic noise since it is present even when N is very large, as shown in Figure 4 (where $N = 1024$). Yet, due to their small size, these emerging incoherent spatio-temporal structures are prone to be affected by demographic fluctuations and result in being noisy. In regime (ii), the spiral waves' wavelengths, λ_H (7) near the HB and $\lambda_{\mu \ll \mu_H}$ (8) at low mutation rate, are much larger than the inter-patch space and smaller than the domain size. Hence, stable spiraling patterns fit within the lattice and are similar to those predicted by the PDEs (4), see Figure 4 (bottom left). In regime (iii), the predicted λ_H and $\lambda_{\mu \ll \mu_H}$ outgrow the lattice and the arms of the resulting large spirals appear like planar waves, see Figure 4 (bottom right). Interestingly, planar waves have been found in the model of Ref. [42] without mutations ($\mu = 0$) at sufficiently high pair-exchange rate.

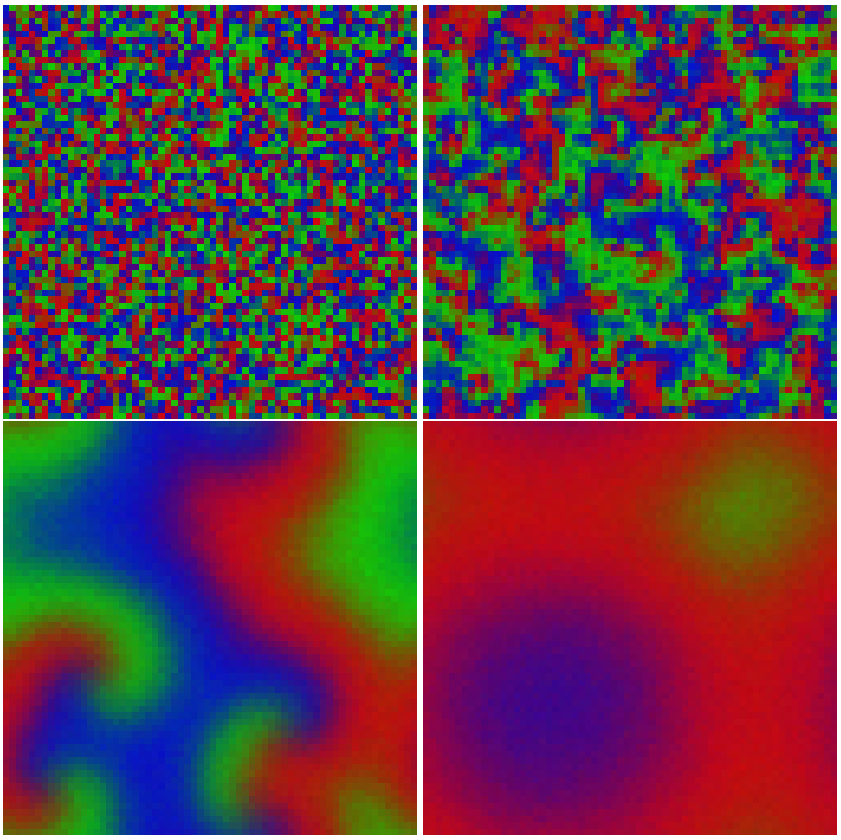

Figure 4. Typical snapshots of stochastic simulations of the model with $(\beta, \sigma, \zeta, \mu) = (1, 1, 0.6, 0.01)$, $N = 1024$ and $L = 64$ and different mobility rates after a time $t = 200$. The mobility rate and predicted wavelength are from left to right: $(\delta, \lambda) = (0.000625, 1)$ and $(\delta, \lambda) = (0.005625, 3)$ in the top row, and $(\delta, \lambda) = (0.64, L/2)$ and $(\delta, \lambda) = (1.44, 3L/4)$ in the bottom row, see text. Adapted from [47].

In order to estimate the boundaries between these regimes, we can use the relations (7) and (8) in the BS phase. According to those, $\lambda = \kappa\sqrt{\delta}/\epsilon$, where $\kappa = 2\pi/\sqrt{1 - R^2(c)}$ is a constant such $15.7 \lesssim \kappa \lesssim 28.1$. Hence, the regime (i) corresponds to low mobility rates of order $\delta \sim o(\epsilon^2)$; in regime (ii) we have $\epsilon^2 \ll \delta \lesssim (L\epsilon/\kappa)^2$ (intermediate mobility rate); while in regime (iii) $\delta \gtrsim (L\epsilon/\kappa)^2$ (high mobility rate), as summarized in the following table where we have also included the corresponding diffusion coefficient $D = \delta/L^2$ on a domain of unit size ($\mathcal{S} = 1$):

Table 1. Spatio-temporal patterns emerging in three different regimes, at low (i), intermediate (ii) and high (iii) mobility rate.

Wavelength λ	*Mobility Rate* δ	*Diffusion Coefficient* D ($\mathcal{S} = 1$)	*Patterns on Grid*
$\lambda \sim \mathcal{O}(1)$	$\delta \sim o(\epsilon^2)$	$D \sim o((\epsilon/L)^2)$	Clumps of activity
$1 \ll \lambda \lesssim L$	$\epsilon^2 \ll \delta \lesssim (L\epsilon/\kappa)^2$	$(\epsilon/L)^2 \ll D \lesssim (\epsilon/\kappa)^2$	Stable spirals
$\lambda \gtrsim L$	$\delta \gtrsim (L\epsilon/\kappa)^2$	$D \gtrsim (\epsilon/\kappa)^2$	Planar waves

This means that stable spirals of wavelength given by (7) or (8) can be observed in the BS phase in the range of mobility rate $\epsilon^2 \ll \delta \lesssim (L\epsilon/\kappa)^2$ that grows with L. Hence, when L is sufficiently large lattice simulations will lead to the formation of stable spiral waves almost for any finite mobility rate. However, as the size of plates used in most microbial experiments rarely exceeds $L = 100$ [6], it is interesting to consider the case where L is not too large. In particular, when the ratio $L/\kappa = \mathcal{O}(1)$, the range $\epsilon^2 \ll \delta \lesssim (L\epsilon/\kappa)^2$ is finite and spiral waves outgrow the lattice even for a finite mobility rate $\delta \gtrsim (L\epsilon/\kappa)^2$. For instance, in Figure 4, we have $L = 64$ and $(\beta, \sigma, \zeta, \mu, \delta, N, L) = (1, 1, 0.6, 0.01, 1024)$

which yields $\epsilon \approx 0.3$, $c \approx 1.0$, $R^2 \approx 0.9$ [45,47], and $L\epsilon/\kappa \approx 0.92$. In this example, with (7) and (8) we find $\lambda(\delta = 0.64) = L/2$ and $\lambda(\delta = 1.44) = 3L/4$. According to the above discussion we expect to find visible spiral waves for $\delta = 0.64$ and patterns resembling planar waves when $\delta = 1.44$ which is confirmed by the bottom row of Figure 4. For the example of Figure 4, the PDEs (4) predict the formation of small spiral waves of wavelength $\lambda = 1$ and $\lambda = 3$ for $\delta = 0.000625$ and $\delta = 0.005625$ respectively, which result in the noisy clumps of activities on the lattice of the top panel of Figure 4.

4.2. Far-Field Breakup of Spiral Waves under Weak Pair-Exchange Rate

Variants of the two-dimensional RPS model (1)–(3) without mutation ($\mu = 0$) have received significant interest and many authors have studied under which circumstances the dynamics leads to the formation of stable spiraling patterns, see, e.g., [24–26,28,30,32,35–38,41]. In Refs. [24–26], where only the dominance-removal was considered, it was found that the cyclically competing populations moving under pair-exchange always form persisting spiraling patterns under a critical mobility threshold whereas no such coherent patterns were found in a similar system where the cyclic competition was implemented according to the dominance-replacement process, see, e.g., [28,31,37]. By means of an approximate mapping onto a CGLE, the authors of Ref. [28] concluded that while the model with dominance-removal ($\sigma > 0$, $\zeta = 0$) can sustain spiral waves, this is not the case of models with dominance-replacement ($\sigma = 0$, $\zeta > 0$). In Ref. [41], it is found that the combination dominance-removal and dominance-replacement processes can lead to stable spiraling patterns as well as to convectively unstable spiral waves. This picture was complemented and unified in our recent work [43,45–47] where these questions were considered in the presence/absence of a small mutation rate and *nonlinear mobility* (pair-exchange and hopping processes were divorced). In particular, we showed that when the mutation rate is low or vanishes, *nonlinear mobility* alters the stability of the spiral waves and is responsible for their far-field breakup.

In this section we report that a similar intriguing phenomenon also occurs in the case where the mobility of the individuals is implemented by the simple nearest-neighbor pair-exchange (3) which result in *linear diffusive terms* in the corresponding PDEs (4). To characterize this novel phenomenon we have implemented the cyclic dominance by considering only dominance-removal, i.e., we have set $\sigma = \beta = 1$ and $\zeta = \mu = 0$, and let the pair-exchange rate δ vary. This variant of the model is therefore the metapopulation version (here $N = 1024$) of the model considered, e.g., in [24–26,28] (where $N = 1$). Based on these previous works, see, e.g., [24–26,28,43,45], we would anticipate that the dynamics of such a variant of the model would be characterized by the formation of stable spiral waves. As shown in Figure 5 (top, left), this is indeed the case when the pair-exchange is sufficiently high ($\delta = 0.4$). However, when δ is lowered the spiral waves become *far–field unstable*, see Figure 5, after the shortening of their wavelength according to the scaling $\lambda \sim \sqrt{\delta}$. Hence, as the wavelength is reduced under low mobility, it appears that the core of the spirals can sustain its arms only for a few rounds before a convective instability starts growing, very much like in the EI phase, and eventually cause the far-field breakup of the spiral waves. While the detailed mechanism of this far-field breakup has still to be elucidated, we believe that it stems from the nonlinear nature of the problem since demographic noise is not at its origin (for $N = 1024$ fluctuations are here negligible). We also think that a spiral far-field breakup always arises when $\zeta \approx 0$ and $\mu = 0$, but depending on the mobility rate δ it occurs outside the lattice (high mobility rate) or within the grid (low mobility rate). In fact, a careful analysis of the PDEs (4) explains this phenomenon of far-field breakup with $\mu = 0$: For fixed $\sigma > 0$, spiral waves exhibit far-field breakup when $\zeta \gtrsim \sigma/2$ or when ζ is close to zero. However, this analysis is beyond the scope of this paper and will be given elsewhere [63].

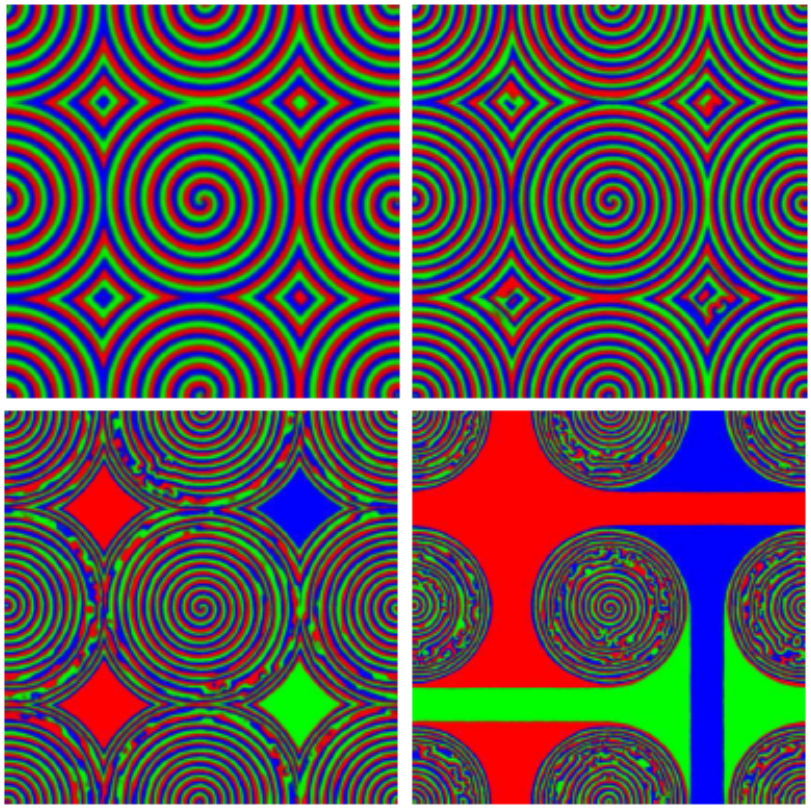

Figure 5. (Color online). Typical snapshots of stochastic lattice simulations of the model with $(\beta, \sigma, \zeta, \mu) = (1, 1, 0, 0)$, $N = 256$ and $L = 512$ and different mobility after a time $t = 800$. In each panel, the initial condition (geometrically ordered and partially visible in the bottom right panel) is the same. The mobility rate is from left to right: $\delta = 0.4$ and $\delta = 0.2$ in the top row, and $\delta = 0.1$ and $\delta = 0.05$ in the bottom row. Adapted from [47].

5. Summary and Conclusions

We have studied the influence of a simple form of mobility, modeled by a pair-exchange between nearest neighbors, on the spatio–temporal patterns emerging in the generic two-dimensional model of [43,45] for the cyclic rock-paper-scissors competition between three species. The underlying evolutionary processes are cyclic dominance–removal and cyclic dominance–replacement interactions, reproduction, migration (pair-exchange), and mutation. While various properties of this system, formulated as a metapopulation model, were investigated in [43,45] by combining multiscale and size expansions with numerical simulations, here we have analyzed the influence of the simple pair-exchange process on the properties of the spiraling patterns characterizing the dynamics of this system.

First, we have highlighted resolution issues that arise on finite lattices: While the description of the dynamics in terms of the underlying partial differential equations predict the formation of spiraling patterns in the so-called "bound-state phase", spiral waves may simply be elusive in the simulations on a finite lattice if the mobility rate is too low. More precisely, when the size of the lattice is finite and comparable to the size of experimental plates, we show that well-defined spiral waves can be observed only when the mobility rate is within a finite range: When the mobility rate is too low, the PDEs predict the emergence of spiral waves of wavelength of order of the lattice spacing which cannot be resolved, whereas when the mobility rate is sufficiently high the resulting spiraling patterns have a wavelength of the order of the lattice size and appear like planar waves. Spiral waves can be observed in lattice simulations when the mobility rate is between these two values. In fact, building on the

analysis carried out in Refs. [43,45] in terms of the system's complex Ginzburg-Landau equation, we have estimated the critical value of the mobility rate. While the range within which spiral waves in bound-state phase grows with the size of the system, we have found that such a range may be finite and therefore spiraling patterns too small to be resolved and observable on lattices of a size comparable to the plates used in most experiments (96-well plates, see, e.g., [8]). We believe that these "resolution issues" may therefore be particularly relevant when one tries to interpret experimental results and can explain why spiral waves appear to be elusive in microbial experiments as those of [6,8].

Second, we have focused on the version of the model with cyclic dominance–removal and without mutations that has received significant attention in the recent years, see, e.g., [24–26]. While previous works reported that in this case the underlying rock-paper-scissors dynamics (with $\zeta = \mu = 0$) leads to well-defined spiraling patterns, here we show that spiraling patterns become convectively unstable and that a far-field breakup occurs when the mobility rate is lowered (with the other rates kept constant). We have verified that the mechanism underlying this phenomenon does not originate from demographic fluctuations and refer to the future work for a detailed analysis of its mechanism in terms of the system's partial differential equations [63].

While we have specifically discussed the biologically-relevant case of the two-dimensional metapopulation model, this analysis can be readily extended to one-dimensional and three-dimensional lattices on which we would respectively expect traveling and scroll waves instead of spiral waves. It would also be interesting to study whether similar phenomena would arise to the oscillating patterns characterizing some RPS games on small-world networks [64–66].

Acknowledgments: The support to BS via an EPSRC Ph.D. studentship (Grant No. EP/P505593/1) is gratefully acknowledged.

Author Contributions: M.M. has written the paper with inputs from A.M.R. and B.S. B.S. has performed the computer simulations and prepared the figures. All authors have discussed and analyzed the results.

Conflicts of Interest: The authors declare no conflict of interest.

References

1. Pennisi, E. What Determines Species Diversity? *Science* **2005**, *309*, 90.
2. Hofbauer, J.; Sigmund, K. *Evolutionary Games and Population Dynamics*; Cambridge University Press: Cambridge, UK, 1998.
3. Nowak, R.M. *Evolutionary Dynamics*; Belknap Press: Cambridge, MA, USA, 2006.
4. Frey, E. Evolutionary game theory: Theoretical concepts and applications to microbial communities. *Phys. A* **2010**, *389*, 4265–4298.
5. Sinervo, B.; Lively, C.M. The rock-paper-scissors game and the evolution of alternative male strategies. *Nature* **1996**, *380*, 240–243.
6. Kerr, B.; Riley, M.A.; Feldman, M.W.; Bohannan, B.J.M. Local dispersal promotes biodiversity in a real-life game of rock-paper-scissors. *Nature* **2002**, *418*, 171–174.
7. Kerr, B.; Neuhauser, C.; Bohannan, B.J.M.; Dean, A.M. Local migration promotes competitive restraint in a host-pathogen 'tragedy of the commons. *Nature* **2006**, *442*, 75–78.
8. Nahum, J.R.; Harding, B.N.; Kerr, B. Evolution of restraint in a structured rock-paper-scissors community. *Proc. Natl. Acad. Sci. USA* **2011**, *108*, 10831–10838.
9. Sinervo, B.; Miles, D.B.; Frankino, W.A.; Klukowski, M.; DeNardo, D.F. Testosterone, Endurance, and Darwinian Fitness: Natural and Sexual Selection on the Physiological Bases of Alternative Male Behaviors in Side-Blotched Lizards. *Horm. Behav.* **2000**, *38*, 222–233.
10. Jackson, J.B.C.; Buss, L. Allelopathy and spatial competition among coral reef invertebrates. *Proc. Nat. Acad. Sci. USA* **1975**, *72*, 5160–5163.
11. Frean, M.; Abraham, E.D. Rock-scissors-paper and the survival of the weakest. *Proc. R. Soc. Lond. B* **2001**, *268*, 1323–1327.
12. Ifti, M.; Bergensen, B. Survival and extinction in cyclic and neutral three–species systems. *Eur. Phys. J. E* **2003**, *10*, 241–248.

13. Reichenbach, T.; Mobilia, M.; Frey, E. Coexistence versus extinction in the stochastic cyclic Lotka-Volterra model. *Phys. Rev. E* **2006**, *74*, 051907.
14. Reichenbach, T.; Mobilia, M.; Frey, E. Stochastic effects on biodiversity in cyclic coevolutionary dynamics. *Banach Cent. Publ.* **2008**, *80*, 259–264.
15. Berr, M.; Reichenbach, T.; Schottenloher, M.; Frey, E. Zero-One Survival Behavior of Cyclically Competing Species. *Phys. Rev. Lett.* **2009**, *102*, 048102.
16. Müller, A.P.O.; Gallas, J.A.C. How community size affects survival chances in cyclic competition games that microorganisms play. *Phys. Rev. E* **2010**, *82*, 052901.
17. Turing, A.M. The Chemical Basis of Morphogenesis. *Phil. Trans. R. Soc. B* **1952**, *237*, 37–72.
18. Murray, J.D. *Mathematical Biology*; Springer-Verlag: New York, NY, USA, 1993.
19. Koch, A.J.; Meinhardt, H. Biological pattern formation: From basic mechanisms to complex structures. *Rev. Mod. Phys* **1994**, *66*, 1481–1507.
20. Levin, S.A.; Segel, L.A. Hypothesis to explain the origin of planktonic patchness. *Nature* **1976**, *259*, 659–663.
21. Hassel, M.P.; Comins, H.N.; May, R.M. Species coexistence and self-organizing spatial dynamics. *Nature* **1994**, *370*, 290–292.
22. Maron, J.L.; Harrison, S. Spatial pattern formation in an insect host-parasitoid system. *Science* **1997**, *278*, 1619–1621.
23. Kirkup, B.C.; Riley, M.A. Antibiotic-mediated antagonism leads to a bacterial game of rock-paper-scissors in vivo. *Nature* **2004**, *428*, 412–414.
24. Reichenbach, T.; Mobilia, M.; Frey, E. Mobility promotes and jeopardizes biodiversity in rock-paper-scissors games. *Nature* **2007**, *448*, 1046–1049.
25. Reichenbach, T.; Mobilia, M.; Frey, E. Noise and correlations in a spatial population model with cyclic competititon. *Phys. Rev. Lett.* **2007**, *99*, 238105.
26. Reichenbach, T.; Mobilia, M.; Frey, E. Self-organization of mobile populations in cyclic competititon. *J. Theor. Biol.* **2008**, *254*, 368–383.
27. May, R.M.; Leonard, W.J. Nonlinear aspects of competition between three species. *SIAM J. Appl. Math.* **1975**, *29*, 243–253.
28. Peltomäki, M.; Alava, M. Three-and four-state rock-paper-scissors games with diffusion. *Phys. Rev. E* **2008**, *78*, 031906.
29. Jiang, L.; Zhou, T.; Perc, M.; Huang, X.; Wang, B. Emergence of target waves in paced populations of cyclically competing species. *New J. Phys.* **2009**, *11*, 103001.
30. He, Q.; Mobilia, M.; Täuber, U.C. Co-existence in the two-dimensional May–Leonard model with random rates. *Eur. Phys. J. B* **2011**, *82*, 97–105.
31. He, Q.; Täuber, U.C.; Zia, R.K.P. On the relationship between cyclic and hierarchical three-species predator-prey systems and the two-species Lotka-Volterra model. *Eur. Phys. J. B* **2012**, *85*, 141–153.
32. Tainaka, K.I. Stationary pattern of vortices or strings in biological systems: Lattice version of the Lotka-Volterra Model. *Phys. Rev. Lett.* **1989**, *63*, 2688–2691.
33. Tainaka, K.I. Vortices and strings in a model ecosystem. *Phys. Rev. E* **1994**, *50*, 3401–3409.
34. Frachebourg, L.; Krapivsky, P.L.; Ben-Naim, E. Segregation in a one-dimensional model of interacting species. *Phys. Rev. Lett.* **1996**, *77*, 2125–2128.
35. Szabó, G.; Szolnoki, A. Three-state cyclic voter model extended with Potts energy. *Phys. Rev. E* **2002**, *65*, 036115.
36. Perc, M.; Szolnoki, A.; Szabó, G. Cyclical interactions with alliance specific heterogeneous invasion rates. *Phys. Rev. E* **2007**, *75*, 052102.
37. He, Q.; Mobilia, M.; Täuber, U.C. Spatial rock-paper-scissors models with inhomogeneous reaction rates. *Phys. Rev. E* **2010**, *82*, 051909.
38. Ni, X.; Wang, W.X.; Lai, Y.C.; Grebogi, C. Cyclic competition of mobile species on continuous space: Pattern formation and coexistence. *Phys. Rev. E* **2010**, *82*, 066211.
39. Venkat, S.; Pleimling, M. Mobility and asymmetry effects in one-dimensional rock-paper-scissors games. *Phys. Rev. E* **2010**, *81*, 021917.
40. Mitarai, N.; Gunnarson, I.; Pedersen, B.N.; Rosiek, C.A.; Sneppen, K. Three is much more than two in coarsening dynamics of cyclic competitions. *Phys. Rev. E* **2016**, *93*, 042408.

41. Reichenbach, T.; Frey, E. Instability of spatial patterns and its ambiguous impact on species diversity. *Phys. Rev. Lett.* **2008**, *101*, 058102.
42. Rulands, S.; Zielinski, A.; Frey, E. Global attractors and extinction dynamics of cyclically competing species. *Phys. Rev. E* **2013**, *87*, 052710.
43. Szczesny, B.; Mobilia, M.; Rucklidge, A.M. When does cyclic dominance lead to stable spiral waves? *EPL (Europhys. Lett.)* **2013**, *102*, 28012.
44. Szczesny, B.; Mobilia, M.; Rucklidge, A.M. Supplementary material: When does cyclic dominance lead to stable spiral waves? Available online: https://dx.doi.org/10.6084/m9.figshare.96949 (accessed on 4 August 2016). doi:10.6084/m9.figshare.96949.
45. Szczesny, B.; Mobilia, M.; Rucklidge, A.M. Characterization of spiraling patterns in spatial rock-paper-scissors games. *Phys. Rev. E* **2014**, *90*, 032704.
46. Szolnoki, A.; Mobilia, M.; Jiang, L.-L.; Szczesny, B.; Rucklidge, A.M.; Perc, M. Cyclic dominance in evolutionary game: A review. *J. R. Soc. Interface* **2014**, *11*, 20140735.
47. Szczesny, B. Coevolutionary Dynamics in Structured Populations of Three Species. Ph.D. Thesis, University of Leeds, Leeds, UK, 2014.
48. Avelino, P.P.; Bazeia, D.; Losano, L.; Menezes, J.; Oliveira, B.F. Junctions and spiral patterns in generalized rock-paper-scissors models. *Phys. Rev. E* **2012**, *86*, 036112.
49. Roman, A.; Dasgupta, A.; Pleimling, M. Interplay between partnership formation and competition in generalized May-Leonard games. *Phys. Rev. E* **2013**, *87*, 032148.
50. Mowlaei, S.; Roman, A.; Pleimling, M. Spirals and coarsening patterns in the competition of many species: A complex Ginzburg-Landau approach. *J. Phys. A: Math. Theor.* **2014**, *47*, 165001.
51. Siegert, F.; Weijer, C.J. Spiral and concentric waves organize multicellular Dictyostelium mounds. *Curr. Biol.* **1995**, *5*, 937–943.
52. Igoshin, O.A.; Welch, R.; Kaiser, D.; Oster, G. A biochemical oscillator explains several aspects of Myxococcus xanthus behavior during development. *Proc. Natl. Acad. Sci. USA* **2004**, *101*, 15760–15765.
53. Hanski, I. *Metapopulation Ecology*; Oxford University Press: New York, NY, USA, 1999.
54. Mobilia, M. Oscillatory dynamics in rock-paper-scissors games with mutations. *J. Theor. Biol.* **2010**, *264*, 1–10.
55. Toupo, D.F.P.; Strogatz, S.H. Nonlinear Dynamics of the Rock-Paper-Scissors Game with Mutations. *Phys. Rev. E* **2015**, *91*, 052907.
56. Gillespie, D.T. A General Method for Numerically Simulating the Stochastic Time Evolution of Coupled Chemical Reactions. *J. Comput. Phys.* **1976**, 22, 403–434.
57. Van Kampen, N.G. *Stochastic Processes in Physics and Chemistry*; Elsevier: Amsterdam, The Netherlands, 1992.
58. Gardiner, C. *Handbook of Stochastic Methods*, 2nd ed.; Springer: Heidelberg, Germany, 1985.
59. Lugo, C.A.; McKane, A.J. Quasicycles in a spatial predator-prey model. *Phys. Rev. E* **2008**, *78*, 051911.
60. Butler, T.; Goldenfeld, N. Robust ecological pattern formation induced by demographic noise. *Phys. Rev. E* **2009**, *80*, 030902.
61. Miller, P. *Applied Asymptotic Analysis, Graduate Studies in Mathematics*; American Mathematical Society: Providence, RI, USA, 2006.
62. Aranson, I.S.; Kramer, L. The world of the complex Ginzburg-Landau equation. *Rev. Mod. Phys.* **2002**, *74*, 99–143.
63. Postlethwaite, C.M.; Rucklidge, A.M. Spirals and heteroclinic cycles in a spatially extended rock-paper-scissors model of cyclic dominance. *Phys. Rev. Lett.*, to be submitted.
64. Szabó, G.; Fáth, G. Evolutionary games on graphs. *Phys. Rep.* **2007**, *446*, 97–216.
65. Perc, M.; Szolnoki, A. Coevolutionary games—A mini review. *BioSystems* **2010**, *99*, 109–125.
66. Szabó, G.; Szolnoki, A.; Izsák, R. Rock-scissors-paper game on regular small-world networks. *J. Phys. A Math. Gen.* **2004**, *37*, 2599–2609.